
Article:
Kumar, N.K., Gopi, R.S., Kuppusamy, R. et al. (4 more authors) (2022) Fuzzy logic-based load frequency control in an island hybrid power system model using artificial bee colony optimization. Energies, 15 (6). 2199.

https://doi.org/10.3390/en15062199

---

energies

MDPI

Article

Fuzzy Logic-Based Load Frequency Control in an Island Hybrid Power System Model Using Artificial Bee Colony Optimization

Neelamsetti Kirn Kumar [1], Rahul Sanmugam Gopi [2], Ramya Kuppusamy [3], Srete Nikolovski [4,*], Yuvaraja Teekaraman [5], Indragandhi Vairavasundaram [6] and Siripireddy Venkateswarulu [7]

1 Department of Electrical and Electronics Engineering, M S RAMAIAH Institute of Technology, Bangalore, Karnataka 560054, India; neelamseeti.kiran@gmail.com
2 Department of Electronics and Communication Engineering, Vel Tech Rangarajan Dr. Sagunthala R&D Institute of Science and Technology, Chennai 600062, India; rahulgopi1993@yahoo.com
3 Department of Electrical and Electronics Engineering, Sri Sairam College of Engineering, Bangalore 562106, India; ramyapks26@gmail.com
4 Power Engineering Department, Faculty of Electrical Engineering, Computer Science and Information Technology, University of Osijek, 31000 Osijek, Croatia
5 Department of Electronic and Electrical Engineering, The University of Sheffield, Sheffield S1 3JD, UK; yuvarajastr@gmail.com
6 School of Electrical Engineering, Vellore Institute of Technology, Vellore 632014, India; arunindra08@gmail.com
7 Department of Electrical and Electronics Engineering, Mother Theresa Institute of Engineering and Technology, Palamaner, Andhra Pradesh 517408, India; chvreddy237@gmail.com
* Correspondence: srete.nikolovski@ferit.hr

Abstract: This study presents the implementation of Artificial Bee Colony (ABC) optimization in an island hybrid power system model using fuzzy logic-based load frequency control. The Island Hybrid Power System considered in this study consisted of various generation units and an energy storage system. The optimized control parameters of PID using ABC were used in an intelligent fuzzy logic controller. The profiles (power & Frequency) of isolated hybrid power system were improved using a Super Conducting Magnetic Energy Storage (SMES) System. Individual controllers were used for wind turbine and diesel generators to control the power output for balancing the demand (frequency change control). Comparative analysis of power and frequency with the help of various classical and intelligent control configurations is presented. The outcome of the study shows that a minimum deviation in frequency and power is obtained through the proposed Intelligent Fuzzy Control approach for the considered isolated power system model.

Keywords: artificial bee colony algorithm; diesel generator; fuzzy logic control; isolated power system; load frequency control

Citation: Kumar, N.K.; Gopi, R.S.; Kuppusamy, R.; Nikolovski, S.; Teekaraman, Y.; Vairavasundaram, I.; Venkateswarulu, S. Fuzzy Logic-Based Load Frequency Control in an Island Hybrid Power System Model Using Artificial Bee Colony Optimization. *Energies* **2022**, *15*, 2199. https://doi.org/10.3390/en15062199

Academic Editors: Edmundas Kazimieras Zavadskas and Marcin Kaminski

Received: 18 January 2022
Accepted: 15 March 2022
Published: 17 March 2022

1. Introduction

The demand for electrical supply has kept increasing for the last decade, and to match this demand, generation should also increase [1]. But the available resources (fossil fuels) for generation are diminishing, and, as well, they have negative impacts on the environment [2]. In addition to this, more than 20 thousand billion Indian people in the globe are still living in island areas. So the major object of this paper is to help generate clean and reliable power for island-areas people with less cost. In developing economies, the use of diesel generators in isolated grids is particularly prevalent in remote, rural areas and communities where such generators are installed [3]. They are also the sole means of producing electricity. The remoteness of the islands and the associated challenge of fuel distribution logistics result in high fuel cost and a low degree of supply protection [4]. Such problems risk the energy and economic stability of the island system. They are of great interest to many of the least established countries situated within this region. The

isolated system presents specific challenges and unique opportunities for renewable energy deployment [5]. Many isolated areas with small population sizes limit the amount of fuel demand because the small geographical scale limits fuel storage. These are some of the reasons wind–diesel is opted for in the case of isolated power systems [6], as well as its viable cost. Hybrid wind–diesel-based power systems are financially feasible for electrical power supply for regions such as islands and hills, where sufficient speed of wind is not available to generate much electric power [7]. Even with the presence of a generation facility, it falls to engineering to guarantee the successful function of the hybrid power system in reliably supplying consumers [8]. It is concluded that the system will be maintained within the tolerable limit for reliable operation of the appliances of consumers. The diesel generator responds to the frequency of AC electricity being produced based on the demand. Wind energy is irregular, and a change in the demand for real power also occurs frequently. It is vital to have an appropriate control method to maintain the availability of energy and nullify the offset between generation and load [9]. Additional power has to be produced immediately once the load is switched on. Generators must automatically decrease their power output when the load is turned off. As consumers turn loads on and off at their convenience, demand keeps changing. When large industrial machinery is powered on or shut down, this can lead to unexpected rises and drops in demand.

To enhance the superiority of the generated power for a continuous supply, this system is combined with a Diesel Engine Generator (DEG) along with an SMES storage device [10]. Modelling and simulation for various hybrid power systems are presented in the literature to control the frequency variations. Frequency control in a power system is controlled using different energy storage systems, such as [11] improvement of inertia enhancement by using SMES, control of a microgrid's battery storage system [12], the droop control approach and the implementation of a two-layered model predictive control [13] by power sharing. In [14] an ultra-capacitor, the double-layered capacitor is used in a solar-based hybrid system to stabilize the frequency. By adding a new system to the original system, the complexity of controlling these system parameters is posing a new challenge to the control engineers. To overcome this issue, intelligent control approaches are employed. In the recent past, several research studies have shown results similar to the optimization techniques for engineering problems, especially in the control design part using heuristic algorithms, such as practical swarm optimization [15], genetic algorithm [16], bacteria foraging optimization [17], seeker optimization [18], cultural optimization [19], cat swarm optimization [20] and grey wolf algorithm [21]. These are being widely used by the research community due to their versatile and flexible nature among the various optimal solutions observed. These techniques result in better performance for the resulting global optimum. The artificial bee colony algorithm was extensively used for optimizing various parameters [22], such as optimizing PID control parameters. Because of its robustness, this algorithm is fruitfully used for various objective problems. The main advantage of adopting a heuristic approach is that it offers a quick solution that is easy to understand and implement. Heuristic algorithms are practical, serving as fast and feasible short-term solutions to planning and scheduling problems. This motivated the authors to use this algorithm in optimizing the PID gains for a fuzzy base PID controller in an isolated power system.

Isolated areas are usually located a distance away from the main power grids, where supplies of electricity rely on diesel generators. Renewable energy sources such as photovoltaic systems (PV) and micro-hydro generators are used in conjunction with diesel generators to reduce fuel cost. However, poor management and coordination of the energy sources may not solve the issue of high fuel consumption. In order to address this effectively, an innovative energy storage system was developed to coordinate with various energy sources to reduce the fuel consumption to a minimum.

Zadeh introduced fuzzy logic in the year 1965 for the application of cellular robotics [23] and since then several types of research have applied this logic [24] to various model-based control systems. It gives an exceptional structure with which to understand the

complete model's uncertainties and obscurity with human thinking and reasoning based on membership functions and linguistic variables. In this manuscript, a comprehensive study of various control configurations with Fuzzy Logic Controller (FLC) was carried out. FLC has gained more attention in recent years for its application to power system operation and control. The flow of this research article is organized as follows: in Section 2, the model of the system is explained in detail; in Section 3, the mathematical model of considered work is formulated; in Section 4, the control approach is described and in Section 5, there is a comparative analysis of the results with different control configurations of P, PI and PID. In the final section, a summary of the whole work is presented. The work flow of this study is represented in Figure 1.

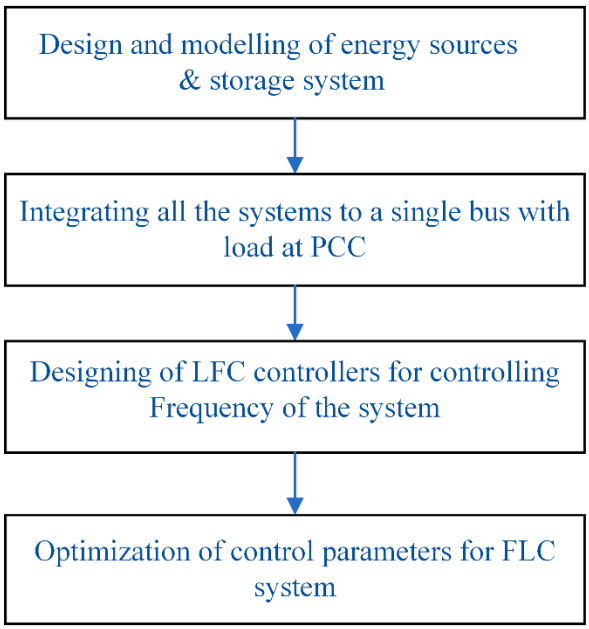

Figure 1. Work flow structure of present study.

2. System Description

Two or more energy generating technologies, from renewable sources such as PV, wind turbines and small hydro turbines, are combined in a traditional hybrid system and from conventional generating sources, usually diesel generators. Moreover, it contains electronics for fuel and batteries for energy storage. In general, hybrid energy systems provide better energy stability because they are connected to multiple sources for enhanced sustainability. These systems are also called green energy integrated systems. Moreover, when run along with a combination of traditional power-generating stations, hybrid systems with RES are also built to satisfy peak demand. A hybrid energy system focused on wind integration and wind power generation with the storage of SMES energy is shown in Figure 2. SMES storage is an electromagnetic mechanism in which electronic converters are energy-charged and stored. Large storage reservoirs can be constructed for this purpose. In the present work, a wind turbine, diesel and SMES storage system were considered for the investigation of LFC with different combinations of fuzzy logic control approaches.

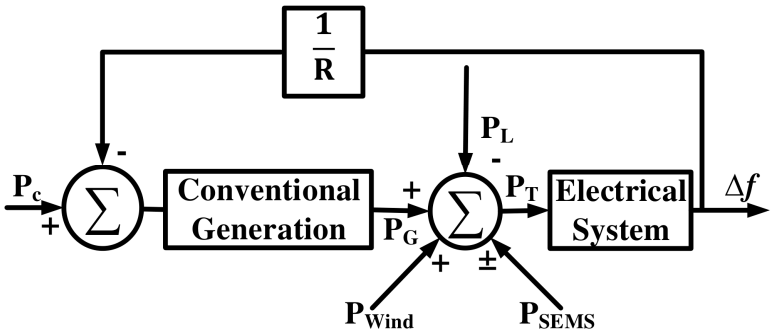

Figure 2. Island hybrid power system model.

3. System Modelling

While modelling the system, certain assumptions were made, such as neglecting the nonlinearities and converters in the system while simulating. This was done with the help of a first-order linear transfer function model. Rated capacities selected for work were wind generation of 150 kW, Diesel of 300 kW and an ESD of 28 kW [10]. The whole structural configuration of an island power system is presented in Figure 3. It consists of DEG, WTG and SMES, having individual controllers for both diesel generators and wind turbines. The simulation parameters considered for the whole system are presented in the next section of the manuscript. The total minor power output increment change (ΔP_{Total}) in the island system is given in the following Equation (1):

$$\Delta P_{Total} = \Delta P_{DEG} + \Delta P_{WTG} \pm \Delta P_{SMES} - \Delta P_L \quad (1)$$

where K_p, K_i, K_v corresponds to proportional, integral and velocity controller gains, respectively. K_{ff} is the feed-forward gain of the system, u, r and y are the control input, reference, and the process output, respectively. ΔP_{DEG} is total power change of diesel generator, ΔP_{WTG} is the total power change (i.e., output of wind turbine) generator, ΔP_{SMES} is the power output change from the SMES storage system and ΔP_L is the load demand change. The system block diagram with transfer function components is shown in Figure 3 and consists of an individual blade pitch control and a load frequency controller. The wind turbine system dynamics are exemplified as a first-order system. The island system may be characterized with the help of state-space representation, as the time dynamics are linear.

$$\dot{X} = [A]X + [B]U + [D]R \quad (2)$$

$$Y = [C]X \quad (3)$$

where 'X' was considered as a state vector, 'U' was considered as a control vector and 'R' was the disturbance vector. Here [A], [B], and [F] are real constant matrices with the same dimensions as state vectors and [Y] is the output vector. For the considered system the state and disturbance vectors are shown in Equations (4)–(7)

$$\dot{X}(t) = \left[\Delta f\ \Delta P_{DEG}\ x_3\ x_4\ \Delta F_T\ x_6\ x_7\ x_8\ \Delta P_{SMES}\ x_{10}\ x_{11}\right] \quad (4)$$

$$U(t) = [U_1\ U_2\ ]^{\mathrm{T}} \quad (5)$$

$$D(t) = [D_1\ D_2\ ] = [\Delta P_L\ \Delta P_{IW}] \quad (6)$$

$$Y(t) = x_1 = \Delta f \quad (7)$$

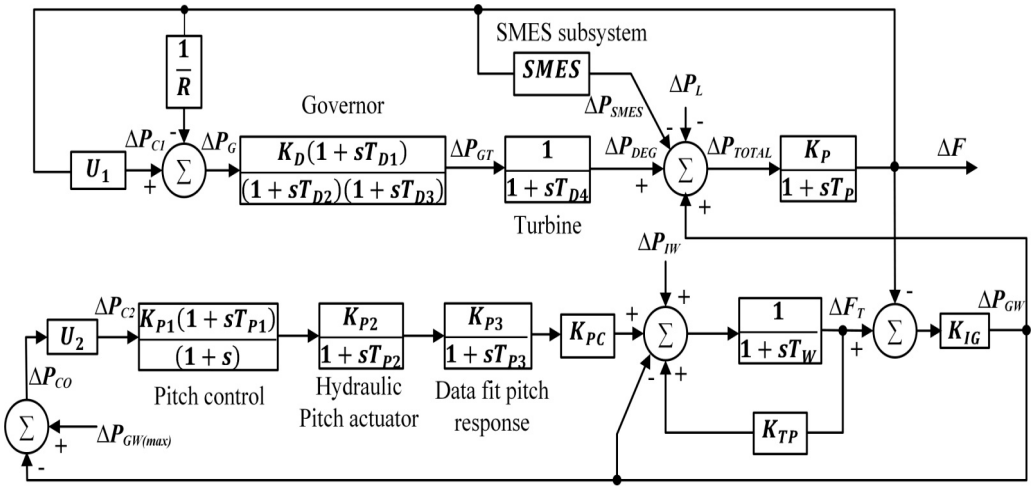

Figure 3. Block diagram of the Island Hybrid Power System.

3.1. Diesel Generator Model

The diesel generator model is a combination of a diesel engine (prime mover) and synchronous generator; it can supply the required power demand based on the rated capacity at a constant frequency. The generator must supply a constant voltage and power according to changes that occurred in the island system, from load fluctuation to wind power fluctuations. The quantity of fuel pumped to the engine with the help of injectors is exclusively responsible for diesel engine speed. The speed of a diesel engine cannot be controlled by the engine itself. It necessitates not only changing engine speed, but also the ability to sustain the desired speed. In its most basic form, a governor is a mechanism that detects and responds to changes in speed. It is built to keep the engine running at the same pace no matter what the load is. The governor of a diesel engine regulates the amount of gasoline injected into the cylinders, hence controlling the engine speed. The governor controller, as shown in Figure 4, is an uncomplicated first-order system, with frequency change of the island system's feed as an input signal.

$$\Delta P_G = \Delta P_{c1} - \frac{\Delta F}{R} \tag{8}$$

$$\Delta P_{c1} = \Delta F[U_1] \tag{9}$$

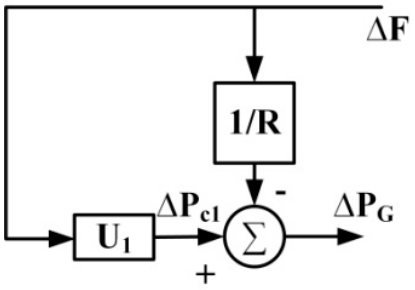

Figure 4. The control block of the governor.

ΔP_G is the change in input to governor, ΔP_{c1} is the output from controller-1 and Δf is the change in frequency.

3.2. Wind Turbine Model

A wind turbine generator (WTG) is a system that converts energy from wind to electrical energy. The operation of a WTG occurs in accordance with this feature because the wind is intermittent. A wind turbine with several blades converts wind energy into mechanical

energy. It is arranged with a fixed gearbox that balances and transfers the turbine's lower speeds to a speed that is required for the generation of power with generators. A blade pitch angle controller is built into the turbines to manage the amount of power that is transformed. An anemometer can be used to measure wind speed. A control technique known as pitch mechanism is the most frequently used technique for regulating the power output of a WTG. When the blades of the turbine exceed the rated speed, the angle of the pitch is reduced to retain the generator output at the rated level. The pitch controller monitors speed control, power making optimization, and the start and halt of the turbine. Pitch control is shown in Figure 5 with a simple first-order model, where the feedback signal is wind turbine power, shown in the equations below.

$$\Delta P_{c0} = \Delta P_{GW(\max)} - \Delta P_{GW} \tag{10}$$

$$\Delta P_{c2} = \Delta P_{c0}[U_2] \tag{11}$$

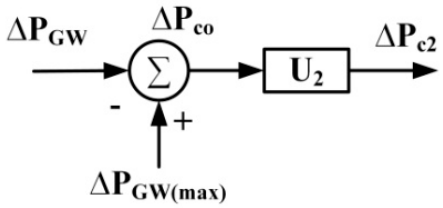

Figure 5. Pitch control block diagram.

ΔP_{c2} is the change in output from controller-2 to wind turbine genetator and ΔP_{c0} is the error signal from wind turbine speed.

3.3. SMES Model

Energy gets stored in the coil as a magnetic field due to the current flow in a superconductor. When this is operated at cryogenic temperatures of 20 K to 77 K, it becomes a superconductor with no resistive losses. It has a more than 98% efficiency rating. The energy storage system is designed with essential parts like superconducting coil, transformer and power training unit, which make up the system. SMES units have additional benefits such as towering power, huge energy density, quick time of response and low-cost maintainance. The superconducting coil charges while in a normal working situation of the power system, since it charges from the AC system. At cryogenic temperatures, the current begins to conduct with fewer electric losses. The governor control and supplemental control respond faster than SMES, and vice versa. The alpha communication angle is used to manage the charge and discharge of the SMES with the help of a converter. If the converter is set to 90, it will operate in charging mode, and if it is set to >90, it will operate in discharge mode. This alpha value control delivers DC voltages in a coil and this must be continuously changed with particular –ve and +ve values.

$$E_d = 2V_{d0}cos\alpha - 2I_dR_c \tag{12}$$

Figure 6 depicts the SMES transfer function model. Change of current through the coil (ΔI_D) is taken as -ve feedback for control of SMES, which improves the capacity of the coil for restoring its current, allowing it to respond promptly to future load disturbances. The equations for change in DC voltage as well as current are shown below in (13) and (14), respectively.

$$\Delta E_D = (-K_{ID}\Delta I_D + K_F\Delta_F)\left(\frac{1}{1+sT_{DC}}\right) \tag{13}$$

$$\Delta I_D = \Delta E_D\left(\frac{1}{sL}\right) \tag{14}$$

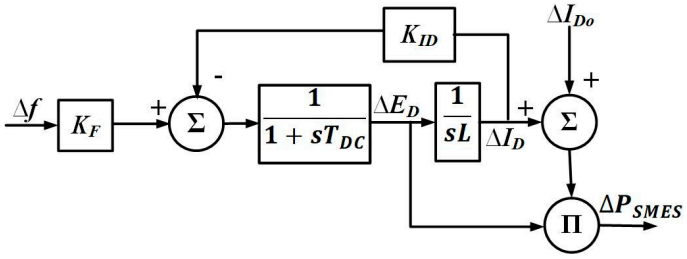

Figure 6. SMES subsystem block.

The real power output from SMES unit is represented below by (15):

$$\Delta P_{SMES} = \Delta E_D I_{D0} + \Delta I_D \Delta E_D \quad (15)$$

ΔE_D—deviation in converter voltage (kV), ΔI_D—change in coil current (kA), L—Inductance of the coil (H) and K_{ID}—feedback gain constant of ΔI_D (kV/kA) K_F—gain constant.

4. Control Methodology

For hybrid power systems, different LFC techniques have been developed. It is possible to classify control methods into various categories such as classical control approaches, adaptive control methods and variable structures, automated control and intelligent control methods. In this section, a complete study of the suggested control techniques for LFC is described.

4.1. Classical Controllers

4.1.1. PI Controllers

The PI control technique was a particular case in a PID controller; where error derivative is not used in the event of data noise, the absence of derivative action will make the system steadier. This is because derivative behaviour in the input to a PI was less sensitive to actual and comparatively rapid changes in the state without derivative intervention. So the system with PI was taking more time to attain a steady-state once subjected to a disturbance, which is represented by Equation (16).

$$G_{PI}(S) = K_P + \frac{K_I}{S} \quad (16)$$

4.1.2. PD Controllers

Derivative controllers respond to change in error signals; however, the response to constant error signal due to zero percent changes over time, for which reason the 'D' derivative control was combined with the 'P' controller. When an error is continuously varying, the output of the controller can differ due to its 'D' action, which is followed by incremental change. This type of controller will cope better with rapid process changes than the P-type control only and will also reduce the steady-state error, just like the proportional control alone, to manage a stable change or a fixed value. This is represented below as Equation (17).

$$G_{PD}(S) = K_P + K_D S \quad (17)$$

4.1.3. PID Controllers

Robust and simple with wide ranges of applicability with near-optimal efficiency, proportional integral derivative (PID) controllers have become numerous and common. They employ techniques widely used in the control process industry. If it is important to boost both systems' transient and steady-state response, neither a PI nor a PD controller can meet the desired requirements. Adding a zero (PD) enhances the transient response but does not increase the form number. The addition of a pole to the origin raises the number

of the form, but even if one zero is added, it can produce an unsatisfactory response time. Two zeros and a pole to the origin are introduced with a proportional-integral-derivative (PID) control.

$$G_{PID}(S) = K_P + \frac{K_I}{S} + K_D S \tag{18}$$

4.2. Performance Parameters

The most likely performance parameters that are commonly used for the validation of the considered control approach are integrated time weight square error (ITSE), integrated squared error (ISE) and integrated absolute error (IAE). These are the most often utilized performance measures. The three performance parameter values are computed with the help of the formula shown in the equations below. The calculated errors for any power system arrangement with the lowest value out of three parameters are regarded as good and are specified by Equations (19)–(21).

$$IAE = \int_0^\infty |\Delta F| dt \tag{19}$$

$$ISE = \int_0^\infty |\Delta F|^2 dt \tag{20}$$

$$ITSE = \int_0^\infty t|\Delta F|^2 dt \tag{21}$$

From the transfer function of the PID controller, all the gains of control parameters are optimized in such a way to achieve better performances. Equations (19)–(21) should have the least values. In the present working model, two individual PID controllers for the diesel generator control (governor control) and the wind turbine control (i.e., pitch control) both have six parameters to be optimized by using the ABC algorithm. It helps to reduce the objective function defined in Equation (19); thus, both power and frequency deviation of the system are reduced and are subject to constraints:

$$\left.\begin{array}{l} K_{Pi}^{min} \le K_{Pi} \le K_{Pi}^{max} \\ K_{Ii}^{min} \le K_{Ii} \le K_{Ii}^{Max} \\ K_{Di}^{min} \le K_{Di} \le K_{Di}^{max} \end{array}\right\}, \; i = 1 \;\&\; 2 \tag{22}$$

where K_{Pi}, K_{Ii}, and K_{Di} are the gains of controller used with FLC, as shown in Equation (22). The equation 'i' represents the corresponding control gain value with minimum and maximum limits, i.e., $0 < K_p, K_I, K_D < 100$.

4.3. Design of Intelligent Controllers

Due to their simple structure, classical controllers such as PI or PID controllers are commonly utilized in the process industry, ensuring proper industrial process performances. These controllers, however, only provide improved performance at fixed operating ranges and need to be returned if the operating range is modified. This provides the impetus for online tuning, where the emphasis is on the automated online synthesis and tuning of traditional controller parameters using online data. The intelligent framework that has been implemented will continually learn to ensure that output targets are met [25]. One of the ways to simplify the role of the operator and to achieve the best output of the controller over a large operating range is the online tuning of a traditional controller via an intelligent method. The FLC has four main blocks, which are fuzzification, fuzzy inference, knowledge base and defuzzification, which are explained in detail. To design an FLC selection of control variables suitably is very important. Commonly, the two inputs for FLC are error and the deviation in error. For selecting the fuzzy parameters such as inputs, membership functions, knowledge-based rules and defuzzification, there is no definite method. But it is difficult to design a rule base, to find the center value of the MFs and its number for FLC. The FLC entails deriving the rule for control using heuristic

(fuzzy) rules [26]. A fuzzification process must be used to fuzzify the input and output signals. A set of fuzzy rules makes up a fuzzy rule foundation. Fuzzy logic provides a systematic methodology for the implementation of heuristic knowledge of humans. Among the various intelligent control techniques, it is regarded as an obvious solution for tuning traditional controllers. The steps to design an FLC structure are shown in Figure 7. The inputs are classified based on one of several linguistic variables, each one with its associated value. Large negative (LN), medium negative (MN), small negative (SN), zero (ZO), small positive (SP), medium positive (MP), and large positive (LP) are the seven linguistic variables employed in this study. Each fuzzy set contains two or more inputs, and one output is triangular (excluding the outer part ones, which are trapezoidal). This if-then rule base is represented in Table 1 and the membership functions are depicted in Figure 8.

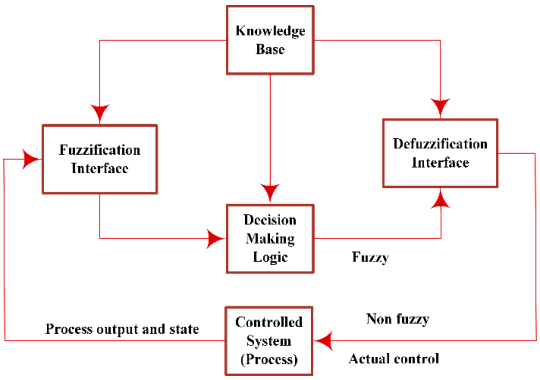

Figure 7. FLC design structure.

Table 1. Parameters of Maglev.

e	$\dot{e}$						
	LN	**MN**	**SN**	**Z**	**SP**	**MP**	**LP**
LN	LP	MP	SP	SP	Z	SP	Z
MN	SP	SP	MP	SP	LN	MN	MN
SN	LP	MP	MP	MP	Z	SN	SN
Z	LN	MN	SN	Z	SN	MP	LP
SP	MP	SP	SP	Z	SP	SP	SP
MP	SP	SP	MP	MP	Z	SN	LN
LP	Z	SP	MP	Z	SN	MN	LN

LN—Large Negative, MN—Medium Negative, SN—Small Negative, Z—Zero, SP—Small Positive, MP—Medium Positive, LP—Large Positive.

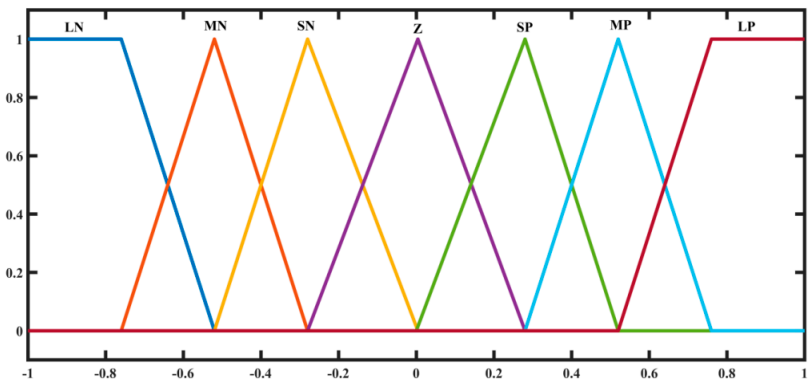

Figure 8. Membership functions designed for ΔF, change in ΔF & FLC output Y.

The error signal or feedback signals ΔF and its change (i.e., derivative error) are considered as the two inputs to the first (FLC U_1) controller and the output is ΔP_{C1} signal passed to the governor of a diesel generator, as shown in Figure 3. The error signal from wind turbine power ΔP_{CO} and its change (i.e., derivative error ΔP_{CO}) are considered as inputs to the second control (U_2) and the output is ΔP_{C2}, the signal passed to the turbine blade pitch control, as shown in Figure 5. The FLCs' outputs, such as P_{C1} and P_{C2}, are utilized to regulate the DG's speed governor and the WTG's blade pitch controller, respectively. These controller rules were established using the "if input-1 & input-2 then output 1" statement.

5. Artificial Bee Colony Optimization

Optimization techniques are currently attracting a huge interest in industrial applications due to their high precision, economy and versatility in producing high quality outputs. In FLC-based PID controllers, optimization techniques were extensively investigated for the tuning of control parameters that result in good performance and reliability.

The ABC method simulates honey bee swarms' intelligent foraging behaviour, and the primary idea in it is to uncover similarities between how bees search for food and how an optimization algorithm finds a solution. The fundamental advantage of the ABC method over other optimization algorithms is that it does both local and global searches in each iteration, increasing the probability of discovering the optimal parameters and avoiding a local optimum to a considerable degree.

The artificial bee colony in the ABC algorithm is made up of three types of bees: employed bees, bystanders and scout bees. Furthermore, the solution is defined by the location of the food sources. The amount of nectar indicates the solution's fitness, and the foraging strategy is governed by three processes: selection, initialization, reproduction, and replacement of bees. The artificial bee colony algorithm flowchart is shown in Figure 9.

In nature, some animals, such as birds, fish, and ants, are skilled at undertaking complex behaviours, which can be described as a collection of small activities carried out by everyone without the need for centralized supervision or monitoring [27]. In a bee colony, the intelligent foraging model is made up of three basic components: food sources, employed foragers, and jobless foragers [28]. In the majority of population-based optimization techniques, a collection of solutions is generated at random and then attempted to be optimized until a certain number of iterations or cycles have been completed.

The algorithm is as follows:

Step1: Set the number of variables, the number of sorts of bees (employers, bystanders, and scooters), and the maximum number of iterations.
Step2: Produce a random solution for the controller parameters like (23) and (24), where X represents the PID scaling factors for each controller in the system:

$$Z = Z_{min} + rand[0\ 1](Z_{max} - Z_{min}) \tag{23}$$

$$Z = \{K_{Pi}, K_{Ii}, K_{Di}\} \text{ where I} = 1\ \&\ 2 \tag{24}$$

Step3: Calculate the objective function based on (19)
Step4: Calculate the relative estimation for the hired bees using the formula in (25), where X_i is the cost function for each employed bee based on (19):

$$F_i = \frac{e^{-X_i}}{average(X_i)} \tag{25}$$

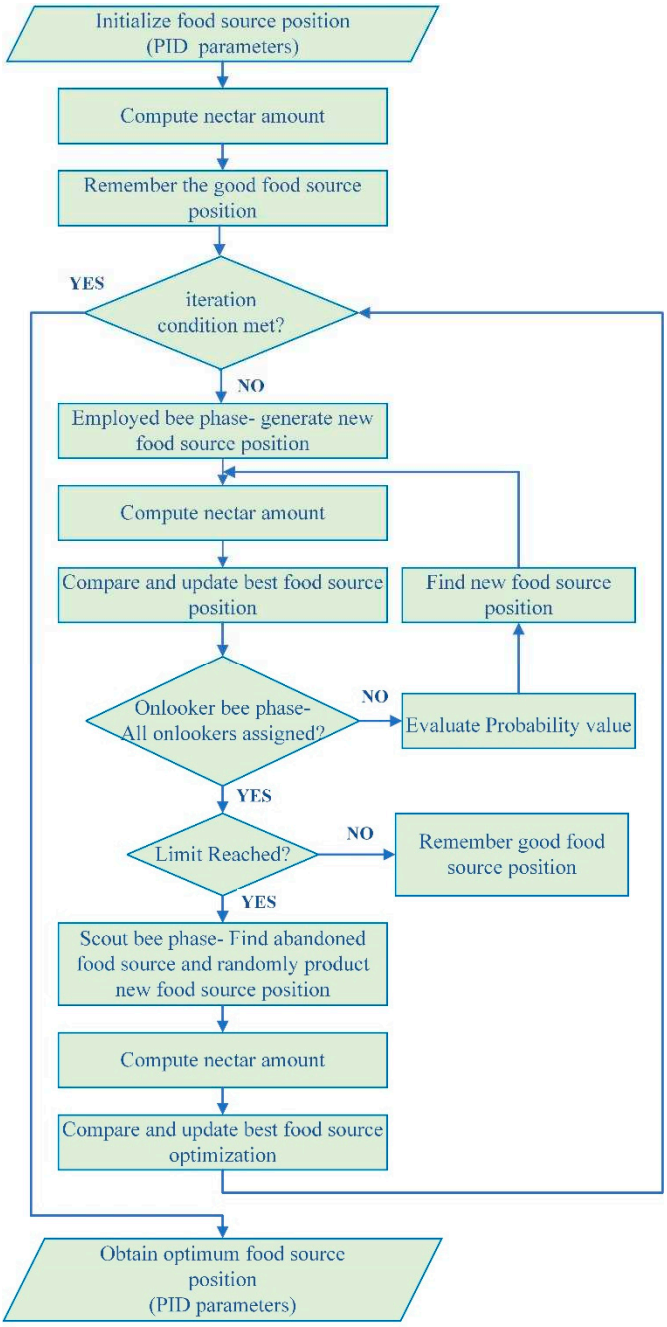

Figure 9. Flow of the algorithm.

Step5: Create a new food location in the same way as in (26), except that s and t are not identical:

$$Z_{new} = Z_{old} + rand[0\ 1](Z_s - Z_t) \tag{26}$$

Step6: Assess the objective function because of the previous criteria: (19).
Step7: Calculate the probability of obtaining a food source, as in (27):

$$P_i = \frac{F_i}{sum(F_i)} \tag{27}$$

Step8: Create a new food source for the observer bees depending on the information provided, as in (27).

Step9: Check with the scout bees to see if there is a previously used solution.
Step10: Select the finest solution that has ever been discovered.
Step11: Has the maximum number of iterations been reached? If this is the case, print the results; otherwise, proceed to step 2.

Initializing the optimization procedure in the ABC algorithm is also committed to the creation of several solutions or food sources at random by dispatching scout bees from colonies [29]. Similarly, because of its capacity to automatically respond to unknown disturbances and model uncertainties that occur in the system, adaptive controllers have gotten a lot of attention [30].

6. Results and Discussions

In the present work, Figure 3 shows PID control techniques for controlling both diesel speed governor and pitch control of wind turbine blades, and in addition with SMES block (i.e, model+ SMES). The state and disturbance vectors are presented in Equations (4) and (6). The real-world island system with quasi-stationary model explicitly states the dependency of wind power variations as disturbance [31]. In the present study, the efficacy of the Artificial Bee Colony optimization algorithm was implemented in optimizing the fuzzy logic control in the studied IHPS with the energy storage system. The IHPS model was tested for different input changes conditions and a random load change condition. These are discussed in the following cases:

Case(i) Performance evolution under a 1% raise in step load demand.
Case(ii) Performance evolution under a 10% and 20% raise in step load demand.
Case(iii) Performance evolution under random raise in load disturbance.

In the present study, different types of inputs and disturbances were considered for simulation and the robustness of the proposed control approach was verified using ABC optimization. The optimal parameter values for both the controllers are depicted in Section 6 for respective load disturbances. FLC was applied to the studied model of IHPS for online real-time application.

6.1. Case (i) Performance Evolution under a 1% Raise in Step Load Demand

The performance of several control combinations (Fuzzy-only, Fuzzy-'PI', Fuzzy 'PD' and Fuzzy-'PID') was analyzed for IHPS at an input step disturbance with an applied increment of 0.01 (1% increase), as shown in Figure 10. The performance results of these control configurations are shown in Figure 11, in which a change in load demand resulted in frequency variation, shown for all four control configurations. The results show that a Fuzzy-'PID' combination reduces the transients and were improved when compared to the remaining control combinations (Fuzzy-only, Fuzzy-'PI', Fuzzy 'PD' and Fuzzy-'PID'). These results are depicted and analyzed by the means of settling time and steady-state error, shown in Tables 2–4. The variation in the power for the load disturbance for these control configurations are also portrayed in Figure 12. At the same time, during the step load disturbance, the change in power in SMES is shown in Figure 13 for all the control configurations. It can be suggested from this curve that the Fuzzy-'PID' combination is much better than the other options.

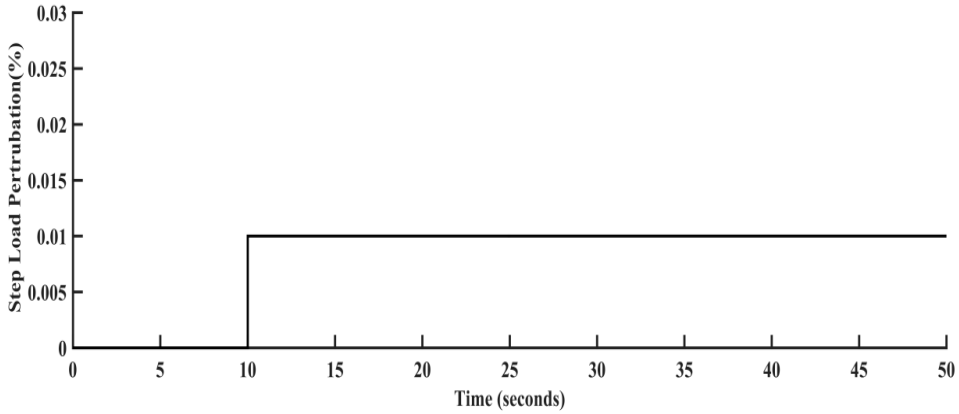

Figure 10. 1% increase in load disturbance.

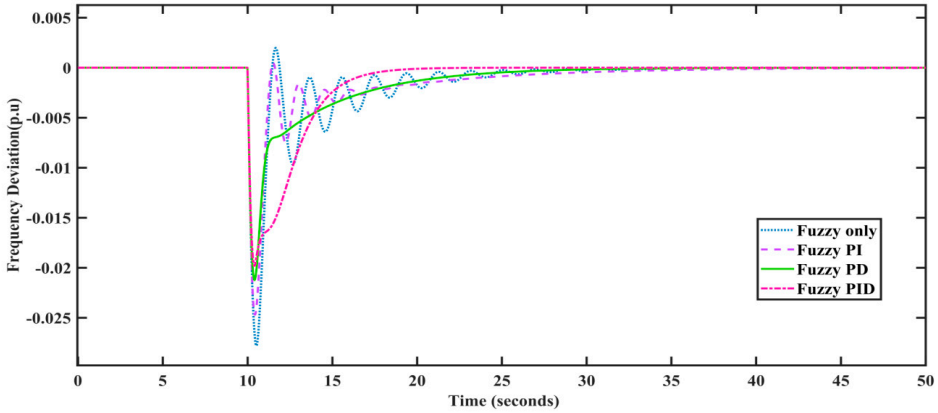

Figure 11. Dynamic response comparison of different control configurations of IHPS frequency change with step input of 1% increase in load.

Table 2. Settling time (seconds) for change in frequency and change in power of the hybrid system with Fuzzy, Fuzzy-'PI', Fuzzy-'PD' and Fuzzy-'PID' against different loads.

Load (p.u)	Change in Frequency (Hz)				Change in Power (p.u)			
	Fuzzy Only	Fuzzy PI	Fuzzy PD	Fuzzy PID	Fuzzy Only	Fuzzy PI	Fuzzy PD	Fuzzy PID
0.01	8.921	8.012	7.421	6.213	9.245	7.012	6.841	5.824
0.1	9.821	7.821	7.423	6.012	9.762	7.121	7.845	6.412

Table 3. Amplitude of oscillations for frequency and power of the hybrid system for Fuzzy, Fuzzy-'PI', Fuzzy-'PD' and Fuzzy-'PID' against different loads.

Load (p.u)	Change in Frequency (Hz)				Change in Power (p.u)			
	Fuzzy Only	Fuzzy PI	Fuzzy PD	Fuzzy PID	Fuzzy Only	Fuzzy PI	Fuzzy PD	Fuzzy PID
0.01	0.0053	0.0048	0.0051	0.0021	0.0024	0.0024	0.0027	0.0009
0.1	0.0281	0.0247	0.0213	0.0191	0.0582	0.0495	0.0467	0.0433

Table 4. The amplitude of oscillations in frequency and power of hybrid system for Fuzzy, Fuzzy-'PI', Fuzzy-'PD' and Fuzzy-'PID' against different loads.

Load (p.u)	Change in Frequency (Hz)				Change in Power (p.u)			
	Fuzzy Only	Fuzzy PI	Fuzzy PD	Fuzzy PID	Fuzzy Only	Fuzzy PI	Fuzzy PD	Fuzzy PID
0.01	0.0018	0.0016	0.0005	-	0.00092	0.00075	0.00022	-
0.1	0.002	0.0012	-	-	0.0081	0.0081	-	-

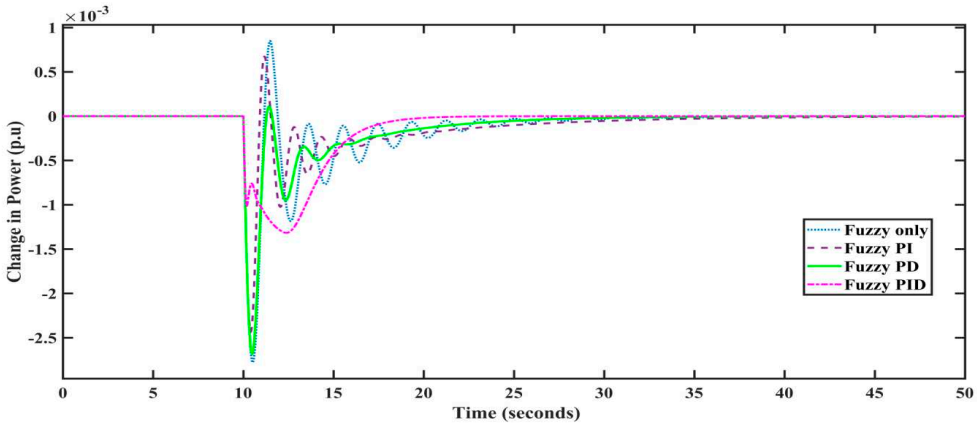

Figure 12. Dynamic response comparison of different control configurations of IHPS power change with step input of 1% increase in load.

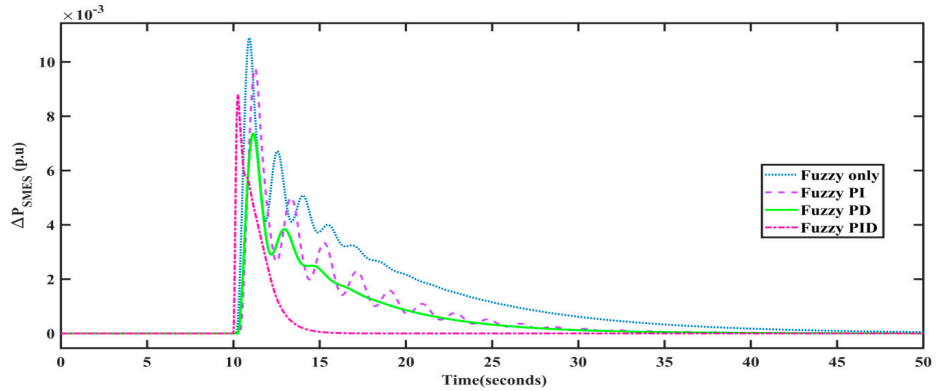

Figure 13. Dynamic response comparison of different control configurations of IHPS SMES power variation with step input of 1% increase in load.

6.2. Case (ii) Performance Evolution under a 10% Raise in Step Load Demand

The performance of several control combinations (Fuzzy-only, Fuzzy-'PI', Fuzzy-'PD' and Fuzzy-'PID') was analyzed for IHPS at an input step disturbance with an applied increment of 0.1 (10% increase). The performance results of these control configurations are shown in Figure 14, in which a change in load demand resulted in frequency variations. This is shown for all four control configurations. The results show that the Fuzzy-'PID' combination reduced the transients and were improved when compared to the remaining control combinations (Fuzzy-only, Fuzzy-'PI', Fuzzy 'PD' and Fuzzy-'PID'). These results are depicted and analyzed by means of the time of settling and steady-state error in Tables 2–4. The variations in the power for the load disturbance for these control configurations are also portrayed in Figure 15. At the same time, during the step load disturbance, the change in power in SMES is shown in Figure 16 for all the control configurations. It can be suggested from this curve that the Fuzzy-'PID' combination is much better than the alternatives. For both cases with step load disturbance of 1% and 10%, the performance

analysis is compared. For better understanding, these are also analyzed using bar charts with respective parameters in Figures 17–19.

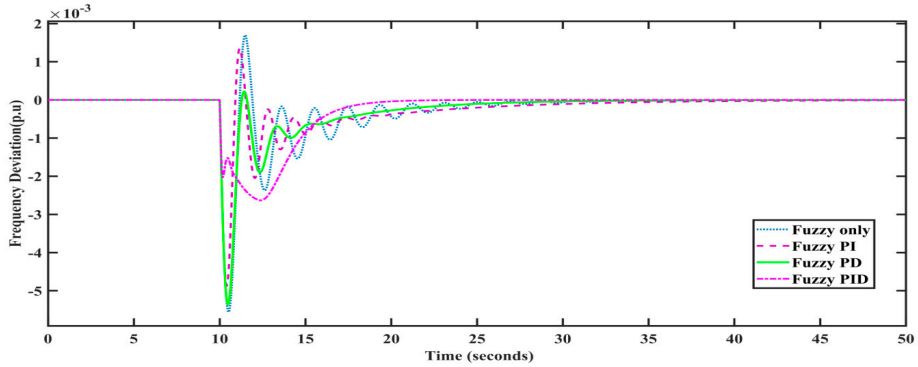

Figure 14. Dynamic response comparison of different control configurations of IHPS frequency change with step input of 10% increase in load.

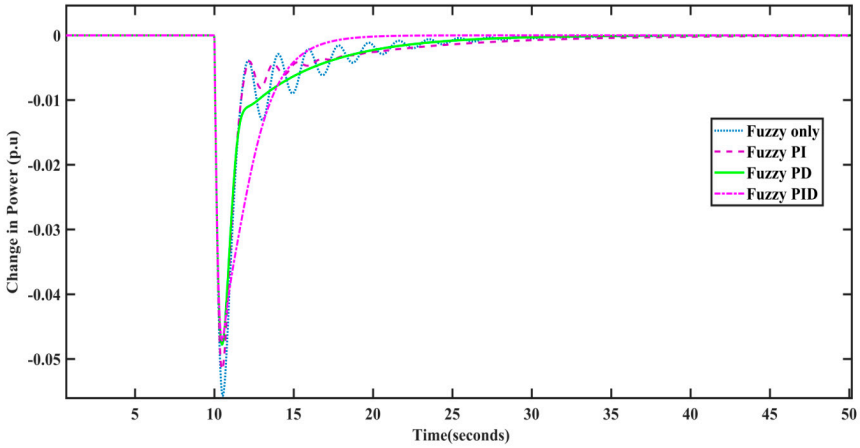

Figure 15. Dynamic response comparison of different control configurations of IHPS frequency change with step input of 10% increase in load.

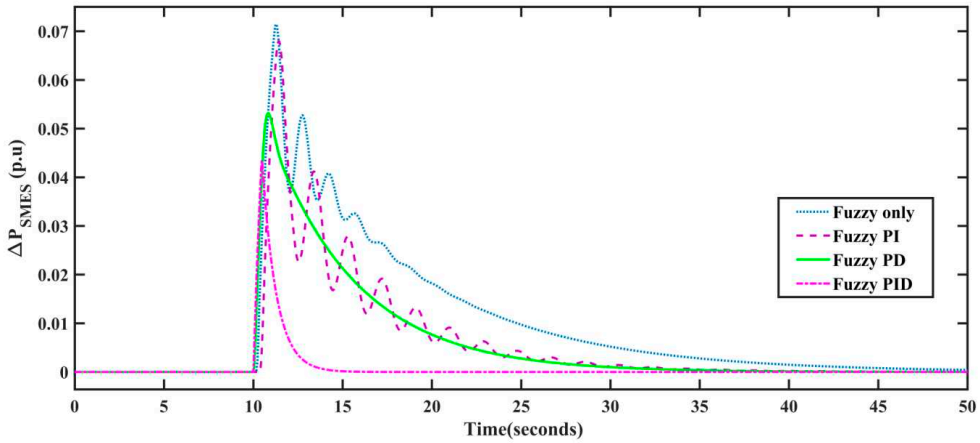

Figure 16. Dynamic response comparison of different control configurations of IHPS SMES power variation with step input of 10% increase in load.

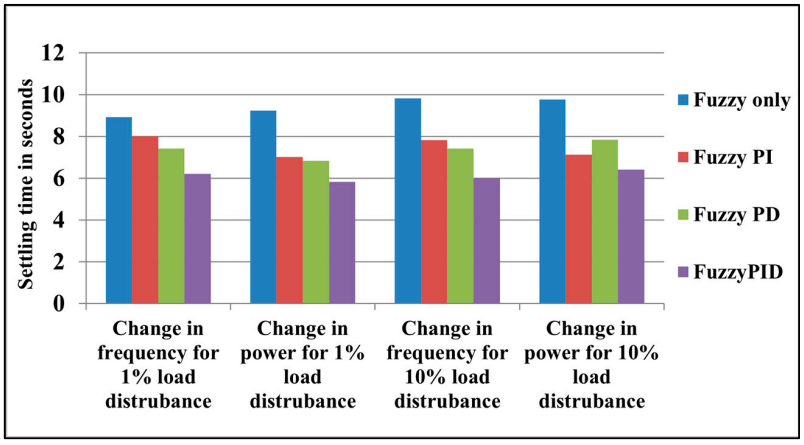

Figure 17. Comparison of dynamic responses of the hybrid system in terms of settling time for frequency and change in power of the hybrid system with Fuzzy, Fuzzy-PI, Fuzzy-PD and Fuzzy -PID against different load disturbances.

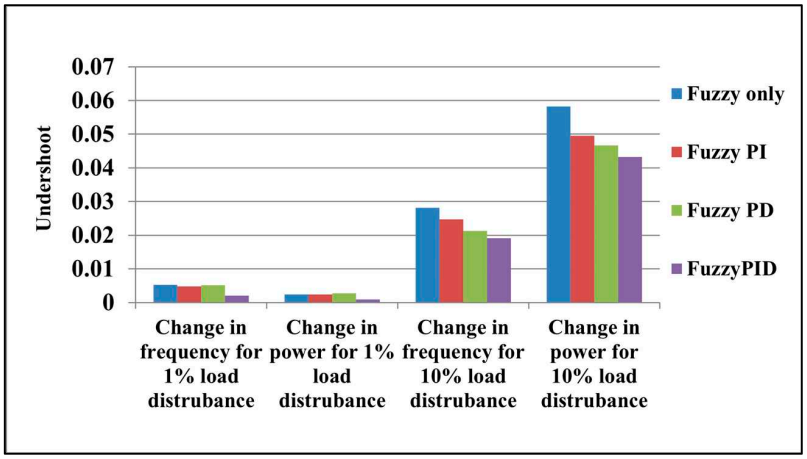

Figure 18. Comparison of dynamic responses of the hybrid system in terms of undershooting (p.u) for frequency and power of the hybrid system with Fuzzy, Fuzzy-'PI', Fuzzy-'PD' and Fuzzy-'PID' against different load disturbances.

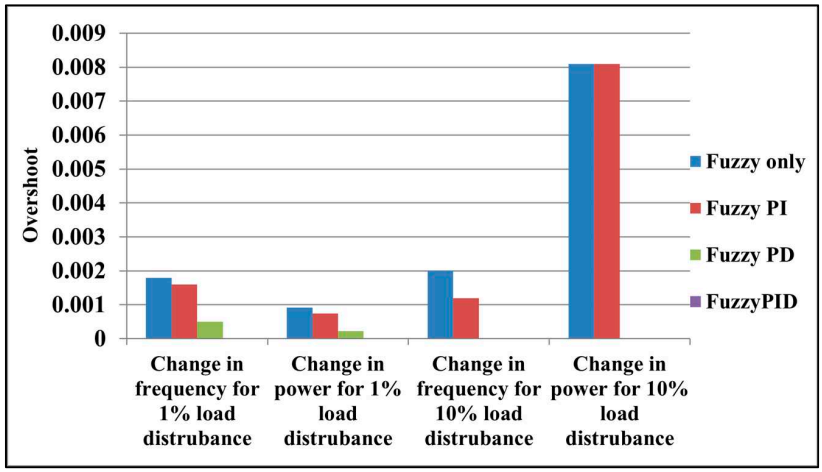

Figure 19. Comparison of dynamic responses of the hybrid system in terms of Overshoot (p.u) for frequency and power of the hybrid system with Fuzzy, Fuzzy-'PI', Fuzzy-'PD' and Fuzzy-'PID' against different load disturbances.

6.3. Case (iii) Performance Evolution under Random Rise in Load Disturbance

The performance of several control combinations (Fuzzy-only, Fuzzy-'PI', Fuzzy 'PD' and Fuzzy-'PID') was analyzed for IHPS at a random input step disturbance at t = 10, 40, 70 and 110 s with an increment of 0.1, −0.2, 0.3 and 0.2 p.u, respectively, applied as depicted in Figure 20. The performance results of these control configurations are shown in Figure 21, which shows that a change in load demand resulted in frequency variation for all four control configurations. The results show that a Fuzzy-'PID' combination reduces the transients and improved when compared to the remaining control combinations (Fuzzy-only, Fuzzy-'PI', Fuzzy 'PD' and Fuzzy-'PID'). These results are depicted and analyzed by the means of the settling time and steady-state error in Tables 5 and 6. The variation in the power for the load disturbance for these control configurations is also portrayed in Figure 22.

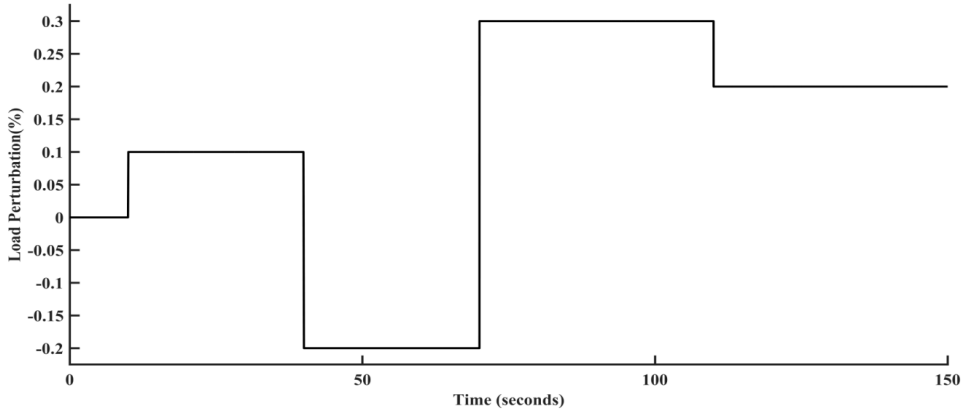

Figure 20. A random load disturbance.

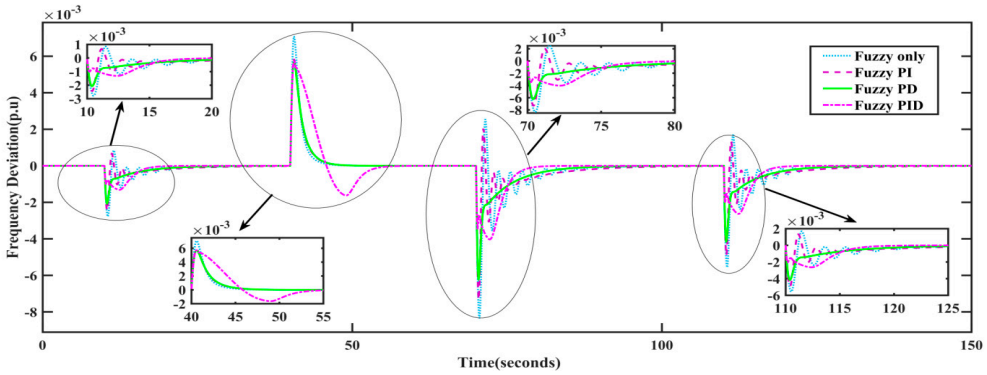

Figure 21. Dynamic response comparison of different control configurations of IHPS frequency change for the random load disturbance.

Table 5. Optimal parameters for both control 1 and 2 using ABC algorithm for Case 1 (1% step change in load).

Controllers	Parameters	Fuzzy-'PI'	Fuzzy-'PD'	Fuzzy-'PID'
Controller-1	K_{P1}	45.2721	89.5956	20.7350
	K_{I1}	87.6931	-	81.8322
	K_{D1}	-	51.5380	21.8282
Controller-2	K_{P2}	12.4553	54.4526	93.7196
	K_{I2}	85.8704	-	32.4170
	K_{D2}	-	60.6446	66.8124

Table 6. Optimal parameters for both control 1 and 2 using ABC algorithm for Case 1 (1% step change in load).

Controllers	Parameters	Fuzzy-'PI'	Fuzzy-'PD'	Fuzzy-'PID'
Controller-1	K_{P1}	94.1045	52.2055	71.2286
	K_{I1}	92.5639	-	45.7883
	K_{D1}	-	52.5204	82.6825
Controller-2	K_{P2}	52.6068	63.7013	81.4496
	K_{I2}	4,300,986	-	42.4122
	K_{D2}	-	9,109,677	93.3730

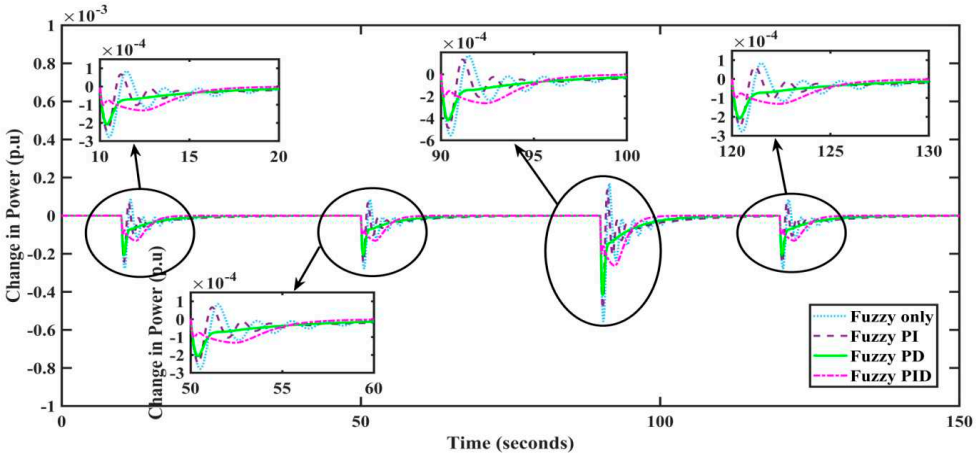

Figure 22. Dynamic response comparison of different control configurations of IHPS change in power for the random load disturbance.

7. Conclusions

The comprehensive study of the IHPS model was investigated for different load disturbances and was carried out with the help of different control configurations. A transient performance analysis using different control configurations comparison was done in this study of IHPS and different step load variations were examined. Here, different case studies were performed to validate the results. A transient study and a performance evaluation of the IHPS with an LFC controller installed on a diesel unit and a turbine blade pitch control mechanism installed on the wind turbine unit has been completed. Instances of wind and diesel units were also studied for the investigation of the outcomes. Using the mathematical model of the controller proposed in this research, the controller gains have been optimized for power system instances under the account of the continuous LFC of the system. The results show that when the system is equipped with a blade pitch control mechanism and LFC for Diesel engine is performing well.

Author Contributions: Conceptualization, N.K.K., S.N., R.S.G., S.V., I.V., Y.T. and R.K.; methodology, N.K.K., S.N., R.S.G., S.V., I.V., Y.T. and R.K.; software, N.K.K., S.N., R.S.G., S.V., I.V., Y.T. and R.K.; validation, N.K.K., S.N., R.S.G., S.V., I.V., Y.T. and R.K.; formal analysis, N.K.K., S.N., R.S.G., S.V., I.V., Y.T. and R.K.; investigation, N.K.K., S.N., R.S.G., S.V., I.V., Y.T. and R.K.; resources, N.K.K., S.N., R.S.G., S.V., I.V., Y.T. and R.K.; data curation, N.K.K., S.N., R.S.G., S.V., I.V., Y.T. and R.K.; writing—original draft preparation, N.K.K., S.N., R.S.G., S.V., I.V., Y.T. and R.K.; writing—review and editing, N.K.K., S.N., R.S.G., S.V., I.V., Y.T. and R.K.; visualization, N.K.K., S.N., R.S.G., S.V., I.V., Y.T. and R.K.; supervision, N.K.K., S.N., R.S.G., S.V., I.V., Y.T. and R.K.; project administration, Y.T.; funding acquisition, S.N. All authors have read and agreed to the published version of the manuscript.

Funding: This research has no external funding.

Informed Consent Statement: Not applicable.

Conflicts of Interest: The authors declare no conflict of interest.

References

1. He, Y.; Guo, S.; Zhou, J.; Wu, F.; Huang, J.; Pei, H. The quantitative techno-economic comparisons and multi-objective capacity optimization of wind-photovoltaic hybrid power system considering different energy storage technologies. *Energy Convers. Manag.* **2021**, *229*, 113779. [CrossRef]
2. Borenstein, S. The Private and Public Economics of Renewable Electricity Generation. *J. Econ. Perspect.* **2012**, *26*, 67–92. [CrossRef]
3. Gatta, F.M.; Geri, A.; Lauria, S.; Maccioni, M.; Palone, F.; Portoghese, P.; Buono, L.; Necci, A. Replacing diesel generators with hybrid renewable power plants: Giglio smart island project. In Proceedings of the 2017 IEEE International Conference on Environment and Electrical Engineering and 2017 IEEE Industrial and Commercial Power Systems Europe (EEEIC/I&CPS Europe), Milan, Italy, 6–9 June 2017; pp. 1–6.
4. Abazari, A.; Monsef, H.; Wu, B. Coordination strategies of distributed energy resources including FESS, DEG, FC and WTG in load frequency control (LFC) scheme of hybrid isolated micro-grid. *Int. J. Electr. Power Energy Syst.* **2019**, *109*, 535–547. [CrossRef]
5. Elkadeem, M.R.; Wang, S.; Azmy, A.M.; Atiya, E.G.; Ullah, Z.; Sharshir, S.W. A systematic decision-making approach for planning and assessment of hybrid renewable energy-based microgrid with techno-economic optimization: A case study on an urban community in Egypt. *Sustain. Cities Soc. J.* **2020**, *54*, 102013. [CrossRef]
6. Sebastián, R.; Peña-Alzola, R. Flywheel Energy Storage and Dump Load to Control the Active Power Excess in a Wind Diesel Power System. *Energies* **2020**, *13*, 2029. [CrossRef]
7. Mbungu, N.T.; Naidoo, R.M.; Bansal, R.C.; Siti, M.W.; Tungadio, D.H. An overview of renewable energy resources and grid integration for commercial building applications. *J. Energy Storage* **2020**, *29*, 101385. [CrossRef]
8. Gawas, N.L.; Shengale, R.; Greene, C.M. Quality Analysis of TAT for Supply Restoration Process. In *IIE Annual Conference. Proceedings*; Institute of Industrial and Systems Engineers: Norcross, GA, USA, 2021; pp. 896–901.
9. Al-Bahrani, L.T.; Horan, B.; Seyedmahmoudian, M.; Stojcevski, A. Dynamic economic emission dispatch with load dema nd management for the load demand of electric vehicles during crest shaving and valley filling in smart cities environment. *Energy* **2020**, *195*, 116946. [CrossRef]
10. Kumar, K.; Gandhi, V.I. Load frequency control for an isolated hybrid power system with hybrid control technique and comparative analysis with different control techniques. *Malay. J. Comput. Sci.* **2020**, 78–92.
11. Rajamand, S. Load frequency control and dynamic response improvement using energy storage and modeling of uncertainty in renewable distributed generators. *J. Energy Storage* **2021**, *37*, 102467. [CrossRef]
12. Sitompul, S.; Fujita, G. Impact of Advanced Load-Frequency Control on Optimal Size of Battery Energy Storage in Islanded Microgrid System. *Energies* **2021**, *14*, 2213. [CrossRef]
13. Oshnoei, A.; Kheradmandi, M.; Muyeen, S.M. Robust Control Scheme for Distributed Battery Energy Storage Systems in Load Frequency Control. *IEEE Trans. Power Syst.* **2020**, *35*, 4781–4791. [CrossRef]
14. Mudi, J.; Shiva, C.K.; Vedik, B.; Mukherjee, V. Frequency Stabilization of Solar Thermal-Photovoltaic Hybrid Renewable Power Generation Using Energy Storage Devices. *Iran. J. Sci. Technol. Trans. Electr. Eng.* **2021**, *45*, 597–617. [CrossRef]
15. Kumar, N.K.; Gandhi, V.I.; Ravi, L.; Vijayakumar, V.; Subramaniyaswamy, V. Improving security for wind energy systems in smart grid applications using digital protection technique. *Sustain. Cities Soc.* **2020**, *60*, 102265.
16. Raja, S.K.; Badathala, V.P.; SS, K. LFC problem by using improved genetic algorithm tuning PID controller. *Int. J. Pure Appl. Math.* **2018**, *120*, 7899–7908.
17. Panwar, A.; Sharma, G.; Bansal, R.C. Optimal AGC design for a hybrid power system using hybrid bacteria foraging optimization algorithm. *Electr. Power Components Syst.* **2019**, *47*, 955–965. [CrossRef]
18. Kumar, M.R.; Deepak, V.; Ghosh, S. Fractional-order controller design in frequency domain using an improved nonlinear adaptive seeker optimization algorithm. *Turk. J. Electr. Eng. Comput. Sci.* **2017**, *25*, 4299–4310. [CrossRef]
19. Pierezan, J.; Maidl, G.; Yamao, E.M.; Coelho, L.d.S.; Mariani, V.C. Cultural coyote optimization algorithm applied to a heavy duty gas turbine operation. *Energy Convers. Manag.* **2019**, *199*, 111932. [CrossRef]
20. Ahmed, A.M.; Rashid, T.A.; Saeed, S.A.M. Cat swarm optimization algorithm: A survey and performance evaluation. *Comput. Intell. Neurosci.* **2020**, *2020*, 4854895. [CrossRef]
21. Paliwal, N.; Srivastava, L.; Pandit, M. Application of grey wolf optimization algorithm for load frequency control in multi-source single area power system. *Evolut. Intell.* **2020**, *15*, 1–22. [CrossRef]
22. Singh, S.; Singh, M.; Kaushik, S.C. Feasibility study of an islanded microgrid in rural area consisting of PV, wind, biomass and battery energy storage system. *Energy Convers. Manag.* **2016**, *128*, 178–190. [CrossRef]
23. Zadeh, L.A. Fuzzy sets. In *Fuzzy Sets, Fuzzy Logic, and Fuzzy Systems: Selected Papers by Lotfi A Zadeh*; World Scientific: Singapore, 1996; pp. 394–432.
24. Feng, G. A survey on analysis and design of model-based fuzzy control systems. *IEEE Trans. Fuzzy Syst.* **2006**, *14*, 676–697. [CrossRef]
25. Ganguly, S.; Mahto, T.; Mukherjee, V. Integrated frequency and power control of an isolated hybrid power system considering scaling factor based fuzzy classical controller. *Swarm Evolut. Comput.* **2017**, *32*, 184–201. [CrossRef]
26. Arya, Y. Improvement in automatic generation control of two-area electric power systems via a new fuzzy aided optimal PIDN-FOI controller. *ISA Trans.* **2018**, *80*, 475–490. [CrossRef] [PubMed]
27. Karaboga, D.; Basturk, B. A powerful and efficient algorithm for numerical function optimization: Artificial bee colony (ABC) algorithm. *J. Global Optim.* **2007**, *39*, 459–471. [CrossRef]

28. Khader, A.T.; Al-betar, M.A.; Mohammed, A.A. Artificial bee colony algorithm, its variants and applications: A survey. *J. Theor. Appl. Inf. Technol.* **2013**, *47*, 434–459.
29. Akay, B.; Karaboga, D. A survey on the applications of artificial bee colony in signal, image, and video processing. *Signal Image Video Process.* **2015**, *9*, 967–990. [CrossRef]
30. Gopi, R.S.; Srinivasan, S.; Panneerselvam, K.; Teekaraman, Y.; Kuppusamy, R.; Urooj, S. Enhanced Model Reference Adaptive Control Scheme for Tracking Control of Magnetic Levitation System. *Energies* **2021**, *9*, 1455. [CrossRef]
31. Ilic, M.; Xie, L.; Liu, Q. (Eds.) *Engineering IT-Enabled Sustainable Electricity Services: The Tale of Two Low-Cost Green Azores Islands*; Springer Science & Business Media: Berlin/Heidelberg, Germany, 2013; Volume 30.